

Theory of light emission from quantum noise in plasmonic contacts: above-threshold emission from higher-order electron-plasmon scattering

Kristen Kaasbjerg^{1,2,*} and Abraham Nitzan²

¹*Department of Condensed Matter Physics, Weizmann Institute of Science, Rehovot 76100, Israel*

²*School of Chemistry, The Sackler Faculty of Exact Sciences, Tel Aviv University, Tel Aviv 69978, Israel*

(Dated: February 24, 2015)

We develop a theoretical framework for the description of light emission from plasmonic contacts based on the nonequilibrium Green function formalism. Our theory establishes a fundamental link between the finite-frequency quantum noise and AC conductance of the contact and the light emission. Calculating the quantum noise to higher orders in the electron-plasmon interaction, we identify a plasmon-induced electron-electron interaction as the source of experimentally observed above-threshold light emission from biased STM contacts. Our findings provide important insight into the effect of interactions on the light emission from atomic-scale contacts.

PACS numbers: 73.63.-b, 72.70.+m, 73.20.Mf, 68.37.Ef

Introduction.—Atomic-size contacts [1], realized, e.g., in scanning tunneling microscopy (STM), provide a unique platform to study fundamental quantum transport phenomena such as, e.g., conductance quantization [2], suppression of shot noise [3], and vibrational inelastic effects on the conductance and shot noise [4, 5]. Recently, light emitted from STM contacts due to inelastic electron scattering off localized plasmons was used as a probe of the shot noise at optical frequencies [6]. Apart from standard emission due to one-electron scattering processes with photon energy $\hbar\omega < eV$, the observation of above-threshold emission with $\hbar\omega > eV$ indicates that interaction effects on the noise are probed [6, 7]. Emission from atomic-scale contacts is thus well-suited for studying the fundamental properties of high-frequency quantum noise.

The role of quantum noise as excitation source of electromagnetic fields is known from theoretical work on mesoscopic conductors [8–11]. The emission is related to the positive frequency part, $\mathcal{S}(\omega > 0)$, of the *asymmetric* quantum shot noise

$$\mathcal{S}(\omega) = \int dt e^{-i\omega t} \langle \delta I(0) \delta I(t) \rangle, \quad (1)$$

where $\delta I = I - \langle I \rangle$ and I is the current operator, whereas the absorption is connected to the negative frequency part, $\mathcal{S}(\omega < 0)$. The study of finite-frequency noise and the associated emission has been attracting attention in atomic-scale [6, 7], molecular [12–16] and mesoscopic conductors [17–27], and may shed light on fundamental issues in molecular optoelectronics [14] and quantum plasmonics [28–30] as well as the origin of above-threshold emission. For the latter, different interactions have been addressed [26, 31–33]. However, a complete picture and a systematic treatment are lacking.

Here, we develop a microscopic theory for plasmonic light emission in atomic-scale contacts based on the Keldysh nonequilibrium Green function (GF) formalism [34, 35]. Our approach allows for a systematic calcu-

lation of the light emission to higher orders in the interaction between the tunnel current and localized surface-plasmon polaritons (LSPs) supported by the contact. LSPs are instrumental to light emission [29, 36–38] and serve as a direct probe of the quantum noise [6] due to their radiative nature and the enhanced electron-plasmon (el-pl) interaction which results from the strong local fields associated with them (see Fig. 1(a)) [39]. We here establish the link between the quantum noise and plasmonic light within the Keldysh GF formalism and furthermore discuss the relation to the AC conductance. Studying a generic contact model, we find that the experimentally observed above-threshold emission [6, 7] stems from higher-order contributions to the quantum noise associated with the plasmon-induced two-electron scattering process illustrated in Fig. 1(b).

Theory.—We consider a single radiative LSP mode with frequency ω_{pl} (see Fig. 1(a)) represented by the quantized vector potential field

$$\mathbf{A}(\mathbf{r}) = \boldsymbol{\xi}_{\text{pl}}(\mathbf{r}) \sqrt{\frac{\hbar}{2\Omega\epsilon_0\omega_{\text{pl}}}} (a^\dagger + a), \quad (2)$$

where Ω is a quantization volume and $\boldsymbol{\xi}_{\text{pl}}$ is a mode vector

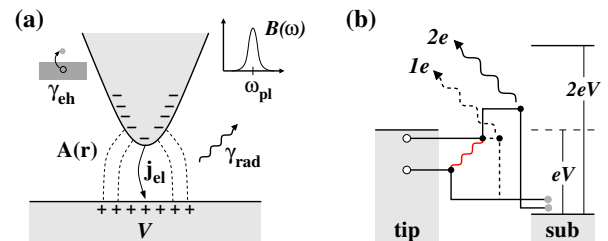


FIG. 1. (Color online) (a) Plasmonic STM contact. The inset illustrates the spectrum of the localized surface-plasmon polarization (LSP) supported by the contact. (b) Schematic illustration of the one and two-electron scattering processes responsible for the $1e$ ($\hbar\omega < eV$; dashed lines) and $2e$ ($eV < \hbar\omega < 2eV$; full lines) light emission.

describing the spatial distribution of the field [40]. The interaction between the LSP and the tunnel current is given by the standard coupling term

$$H_{\text{el-pl}} = \int d\mathbf{r} \mathbf{j}_{\text{el}}(\mathbf{r}) \cdot \mathbf{A}(\mathbf{r}), \quad (3)$$

where $\mathbf{j}_{\text{el}} = \mathbf{j}_{\text{el}}^{\nabla} + \mathbf{j}_{\text{el}}^A$ is the electronic current density, and $\mathbf{j}_{\text{el}}^{\nabla}$ and \mathbf{j}_{el}^A the paramagnetic and diamagnetic components, respectively.

The excitation dynamics of the LSP and the emission is encoded in the LSP GF $D(\tau, \tau') = -i\langle T_c A(\tau) A(\tau') \rangle$ where $A = a + a^\dagger$ and T_c is the time-ordering operator on the Keldysh contour. The retarded and lesser components of the GF are given by their respective Dyson and Keldysh equations,

$$D^r(\omega) = d_0^r(\omega) + d_0^r(\omega) \Pi^r(\omega) D^r(\omega), \quad (4)$$

and

$$D^<(\omega) = D^r(\omega) \Pi^<(\omega) D^a(\omega), \quad (5)$$

where $d_0^r(\omega) = \frac{2\omega_{\text{pl}}}{(\omega + i0^+)^2 - \omega_{\text{pl}}^2}$ is the *bare* GF and $\Pi = \Pi_{\text{el}} + \Pi_{\text{rad}} + \Pi_{\text{eh}}$ is the *irreducible* self-energy which accounts for the interaction with the tunneling current (Π_{el}) as well as radiative decay (Π_{rad}) and decay into bulk electron-hole pair excitation (Π_{eh}). The latter two are modeled with phenomenological damping parameters $\gamma_{\text{rad/eh}}$ with self-energies $\Pi_{\text{rad/eh}}^r(\omega) = -i\gamma_{\text{rad/eh}} \text{sgn}(\omega)/2$ and $\Pi_{\text{rad/eh}}^{>/<}(\omega) = -i\gamma_{\text{rad/eh}} |n_B(\mp\omega)|$, where n_B is the Bose-Einstein distribution function, and give rise to a broadened LSP, $D_0^r(\omega) = \frac{2\omega_{\text{pl}}}{\omega^2 - \omega_{\text{pl}}^2 - i\omega_{\text{pl}}\gamma_0}$, with width $\gamma_0 = \gamma_{\text{rad}} + \gamma_{\text{eh}}$.

The excitation, damping and broadening of the LSP due to the el-pl interaction (3) are governed by the el-pl self-energy, $\Pi_{\text{el}} = \Pi^{\nabla} + \Pi^A$. To lowest order in the interaction, the two contributions are given by [41]

$$\Pi^{\nabla}(\tau, \tau') = -i\langle T_c \delta j(\tau) \delta j(\tau') \rangle_0, \quad (6)$$

and

$$\Pi^A(\tau, \tau') = \delta(\tau - \tau') \langle \rho(\tau) \rangle_0, \quad (7)$$

respectively, where $\delta j = j - \langle j \rangle_0$,

$$j = \sqrt{\frac{\hbar}{2\Omega\epsilon_0\omega_{\text{pl}}}} \int d\mathbf{r} \boldsymbol{\xi}_{\text{pl}}(\mathbf{r}) \cdot \mathbf{j}_{\text{el}}^{\nabla}(\mathbf{r}) \quad (8)$$

is the projection of the current operator onto the LSP mode vector,

$$\rho = -\frac{e^2}{m_e} \frac{\hbar}{2\Omega\epsilon_0\omega_{\text{pl}}} \int d\mathbf{r} \boldsymbol{\xi}_{\text{pl}}(\mathbf{r}) \cdot \boldsymbol{\xi}_{\text{pl}}(\mathbf{r}) \Psi^\dagger(\mathbf{r}) \Psi(\mathbf{r}) \quad (9)$$

is the mode-weighted electron-density operator and $\langle \cdot \rangle_0$ is the expectation value in the absence of the el-pl interaction (3). The diamagnetic self-energy does not affect

the LSP dynamics as it only depends on the static charge density $\langle \rho \rangle_0$, and is here neglected.

From a perturbative expansion of the LSP GF in the paramagnetic interaction, we find that the *exact* paramagnetic self-energy is given by [42]

$$\Pi^{\nabla}(\tau, \tau') = -iS^{\text{irr}}(\tau, \tau'), \quad (10)$$

valid to all orders in the el-pl interaction. Here, S^{irr} is the *irreducible* part of the current-current correlation function $S(\tau, \tau') = \langle T_c \delta j(\tau) \delta j(\tau') \rangle$ [43] and the expectation value $\langle \cdot \rangle$ is with respect to the Hamiltonian that includes the el-pl interaction (3).

Focusing on the case where the el-pl coupling (8) is proportional to the current operator I , the lesser and retarded components of the correlation function S are given by the quantum noise in Eq. (1) and the response function $\mathcal{K}^r(t - t') = -i\Theta(t - t') \langle [I(t), I(t')] \rangle$, respectively. From the important formal result (10), it then follows that the lesser $\Pi^{\nabla, <} = -iS_{\text{irr}}^<$ and retarded $\Pi^{\nabla, r} = -iS_{\text{irr}}^r$ self-energies are directly related to these quantities, thus connecting the damping of the LSP to the dissipative real part of the AC conductance $\mathcal{G}(\omega) = i\mathcal{K}^r(\omega)/\omega$ of the contact. These quantities are connected via [44]

$$-2\omega \text{Re}\mathcal{G} = 2\text{Im}\mathcal{K}^r(\omega) = \mathcal{S}(\omega) - \mathcal{S}(-\omega), \quad (11)$$

which may be regarded as a *nonequilibrium* fluctuation-dissipation relation. This demonstrates a fundamental connection between quantum noise and AC conductance previously discussed in Refs. 8 and 45.

To connect the quantum noise to the light emission, we consider the radiative decay of the LSP into a reservoir of far-field modes, $H_{\text{far-field}} = \sum_{\lambda} \hbar\omega_{\lambda} a_{\lambda}^{\dagger} a_{\lambda}$, with the associated exchange rate per unit frequency given by

$$\Gamma_{\text{rad}}(\omega) = \Pi_{\text{rad}}^<(\omega) D^>(\omega) - \Pi_{\text{rad}}^>(\omega) D^<(\omega). \quad (12)$$

Here, the two terms account for absorption and emission, respectively, in agreement with Eq. (1) [44]. The emitted light is thus governed by $D^<(\omega) = -B(\omega) \frac{\Pi_{\text{el}}^<(\omega)}{2\text{Im}\Pi^r(\omega)} \stackrel{T=0}{\stackrel{\omega>0}{\equiv}} -B(\omega) \frac{\Pi_{\text{el}}^<(\omega)}{2\text{Im}\Pi^r(\omega)}$, where $B = -2\text{Im}D^r$ is the LSP spectral function (see Fig. 1(a)), showing that it resembles the LSP spectrum and is driven by $\Pi_{\text{el}}^<$. With the above, we have established the link between plasmonic light emission and the quantum noise and AC conductance.

Generic model and results.—With the formal theory established, we go on to study the light emission and finite-frequency noise in a generic model for an atomic-scale STM contact consisting of a spin-degenerate electronic state/conduction channel coupled to bulk lead reservoirs of the STM tip and substrate,

$$H = \varepsilon_0 \sum_{\sigma} d_{\sigma}^{\dagger} d_{\sigma} + \sum_{\alpha} H_{\alpha} + H_T + H_{\text{el-pl}} + \hbar\omega_{\text{pl}} a^{\dagger} a. \quad (13)$$

Here, $\varepsilon_0 = 0$ is the energy of the electronic level and $H_{\alpha} = \sum_k \varepsilon_{k,\alpha} c_{k\alpha}^{\dagger} c_{k\alpha}$, $\alpha = \{\text{tip, sub}\}$ is the

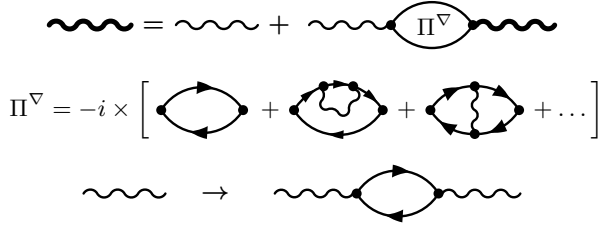


FIG. 2. (Color online) (top) Dyson equation for the LSP GF where Π^∇ denotes the paramagnetic el-pl self-energy. (center) Perturbation expansion of the self-energy showing the diagrams up to 4th order in the el-pl interaction. (bottom) The 6th order diagrams responsible for the $2e$ emission can be obtained by replacing the broadened LSP GF with its 2nd order correction (a plasmon excited by electron tunneling) in the 4th order diagrams. Feynman dictionary: \bullet : el-pl interaction; solid lines: electronic contact GF $G_{ij}(\tau, \tau') = -i\langle T_c c_i(\tau) c_j^\dagger(\tau') \rangle_0$, $i, j = \text{tip, sub, d}$; thin wiggly lines: broadened LSP GF $D_0(\tau, \tau') = -i\langle T_c A(\tau) A(\tau') \rangle_0$.

Hamiltonian of the reservoirs with chemical potentials $\mu_{\text{tip/sub}} = \pm V/2$. The coupling to the reservoirs, $H_T = \sum_{\alpha, k} t_k^\alpha (c_{k\alpha}^\dagger d + \text{h.c.})$, leads to tunnel broadenings $\Gamma_\alpha = 2\pi\rho_\alpha |t_k^\alpha|^2$ which define tunneling ($\Gamma_{\text{sub}} \ll \Gamma_{\text{tip}}$) and contact ($\Gamma_{\text{sub}} \sim \Gamma_{\text{tip}}$) regimes. For $\Gamma = \Gamma_{\text{tip}} + \Gamma_{\text{sub}} \gg eV, k_B T$, the DC conductance is given by $\mathcal{G} = G_0 T$ where $G_0 = 2e^2/h$ and $T = 4\Gamma_{\text{tip}}\Gamma_{\text{sub}}/\Gamma^2$ is the transmission coefficient.

The el-pl interaction takes the form $H_{\text{el-pl}} = \sum_\alpha M_\alpha I_\alpha (a^\dagger + a)$, where $I_\alpha = i\sum_k (t_k c_{k\alpha}^\dagger d - \text{h.c.})$ is the paramagnetic current operator at reservoir α and $M_\alpha = \frac{e}{\hbar} \sqrt{\frac{\hbar}{2\Omega\epsilon_0\omega_{\text{pl}}}} l_\alpha$ is a dimensionless coupling constant with l_α a characteristic length scale for the interaction [46]. To describe the experimental light emission [6, 7], we take the el-pl coupling to be given by $|M_{\text{tip/sub}}| = M$ with $M_{\text{tip}} = -M_{\text{sub}}$, which implies that the LSP couples to the total current $I_{\text{tot}} = I_{\text{tip}} - I_{\text{sub}}$ through the contact [47]. The paramagnetic self-energy can now be written as a sum over lead-lead components, $\Pi^\nabla = \sum_{\alpha\beta} \Pi_{\alpha\beta}^\nabla$, where

$$\Pi_{\alpha\beta}^\nabla(\tau, \tau') = -iM_\alpha M_\beta S_{\alpha\beta}^{\text{irr}}(\tau, \tau'), \quad (14)$$

with $S_{\alpha\beta}(\tau, \tau') = \langle T_c \delta I_\alpha(\tau) \delta I_\beta(\tau') \rangle$ and $\delta I_\alpha = I_\alpha - \langle I_\alpha \rangle$. With the above-mentioned assumption for the coupling constant, we have $\Pi^\nabla(\tau, \tau') = -iM^2 S^{\text{irr}}(\tau, \tau')$ where $S(\tau, \tau') = \langle T_c \delta I_{\text{tot}}(\tau) \delta I_{\text{tot}}(\tau') \rangle$.

In the following, we proceed with a perturbative calculation of the *irreducible* el-pl self-energy illustrated in terms of Feynman diagrams in Fig. 2 (see Ref. [42] for details). We focus on the regime $\Gamma \gg \hbar\omega_{\text{pl}}, eV, k_B T$ and take $k_B T = 0$, corresponding to the experimentally relevant situation $k_B T \ll \hbar\omega_{\text{pl}}$ where the current is the only excitation source for the LSP.

Figure 3(a) shows the numerically calculated (*irreducible*) emission noise to different orders in the el-pl

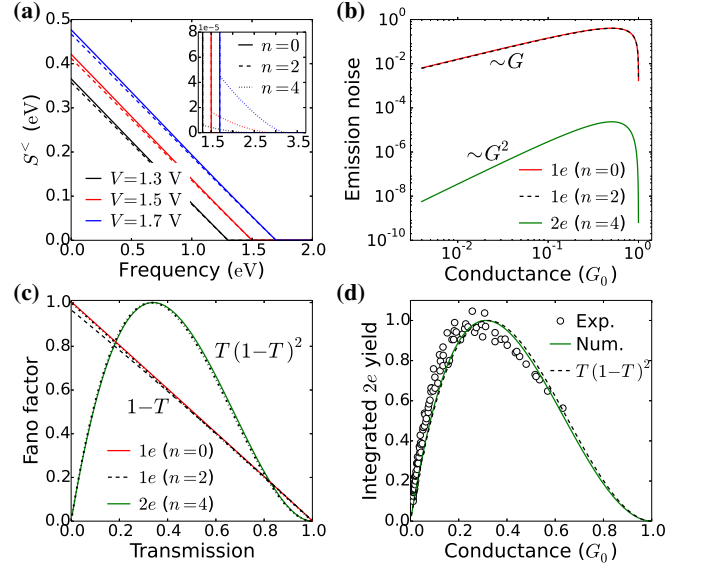


FIG. 3. (Color online) (a) Noise spectrum to different orders in the el-pl interaction ($n = 0$: solid, $n = 2$: dashed, and $n = 4$: dotted lines) for a contact with $T \sim 0.2$. The inset shows a zoom of the noise spectrum at $\omega \gtrsim eV$. (b) and (c) Integrated $1e$ and $2e$ emission noise and Fano factors at $V = 1.6$ V vs conductance and transmission, respectively. The dash-dotted lines in (c) show the indicated analytic functions. (d) Integrated $2e$ emission yield vs conductance at $V = 1.6$ V. The circles show the experimental $2e$ yield from Ref. [6]. In (c) and (d), the Fano factors and yields have been normalized to unity at their maximum value (the $1e$ Fano factors have been normalized with the $n = 0$ maximum). Parameters: $\omega_{\text{pl}} = 1.5$ eV, $\gamma_0 = 0.2$ eV, $M = 0.1$, $\Gamma_{\text{tip}} = 10$ eV.

interaction (the order of the corresponding self-energy is $n + 2$) for a contact with $T \sim 0.2$ and LSP parameters resembling the experiment [6]. The lowest-order ($n = 0$) *noninteracting* quantum noise (full lines in Fig. 3(a)) is given by the *bare* bubble diagram. In the limit $\Gamma \gg eV, \hbar\omega, k_B T$, we find, in agreement with previous works [9, 48], that the *noninteracting* noise spectrum is given by [49]

$$S_0^<(\omega) \approx \frac{4 \times 2}{2\pi} [T(1-T) [H(\omega + eV) + H(\omega - eV)] + 2T^2 H(\omega)], \quad (15)$$

where $H(x) = xn_B(x)$. At $k_B T = 0$, the emission part simplifies to $S_0^<(\omega > 0) \sim T(1-T)\Theta(eV - \omega)(eV - \omega)$, and is hence suppressed at perfect transmission and cut off at $\omega = eV$, i.e. in this order only emission with $\omega < eV$ ($1e$) via the one-electron scattering process illustrated in Fig. 1(b) (dashed lines) is included.

The lowest-order corrections ($n = 2$)—a bubble with a “plasmon-dressed” contact GF and one with a vertex correction—give rise to a reduction of the emission noise (dashed lines in Fig. 3(a)) and are cut off at $\omega = eV$ like the *noninteracting* noise.

The above-threshold emission is contained in the 4th order ($n = 4$) quantum noise. At $k_B T = 0$, it originates from the coherent two-electron scattering process illustrated in Fig. 1(b), which corresponds to a plasmon-induced electron-electron (el-el) interaction. To identify the associated self-energy diagrams we employ the *optical theorem* stating that the imaginary part of a self-energy diagram is given by the sum of squared scattering amplitudes from possible “on-shell” cuts of the self-energy [50]. The relevant self-energy diagrams are therefore identified as the two $n = 2$ diagrams with the damped LSP GF replaced by its lowest-order correction (see bottom Fig. 2). The two diagrams give rise to the $\omega > eV$ component ($2e$) of the noise shown in the inset of Fig. 3(a) (dotted lines) which is cut off at $\omega = 2eV$. The cutoff stems from the above-mentioned scattering process, where an initial emission process exciting the plasmon [wiggly (red) line in Fig. 1(b)] is followed by an absorption process generating a “hot electron” which can emit at above-threshold energies $eV < \omega < 2eV$. At finite temperature, “hot electrons” can also be generated from thermally excited plasmons. However, at $k_B T \ll \hbar\omega_{\text{pl}}$ this process is negligible.

To further analyze the quantum noise, we show in Figure 3(b) the integrated $1e$ ($0 < \omega < eV$) and $2e$ ($eV < \omega < 2eV$) components [6, 7] of the emission noise at $V = 1.6$ V as a function of the conductance. In the tunneling regime, $\mathcal{G} \ll G_0$, the noise components are found to scale with the conductance as $S_{1e}^< \sim \mathcal{G}$ and $S_{2e}^< \sim \mathcal{G}^2$, respectively, emphasizing that they involve one and two-electron scattering processes. Moreover, at perfect transmission, $\mathcal{G} \sim G_0$, both the $1e$ and $2e$ noise are suppressed. For the $1e$ noise, the $n = 2$ corrections do not change this qualitatively. We emphasize that the suppression of emission noise at $T = 1$ only holds in the considered large- Γ limit [42].

The fact that the $2e$ noise shows a \mathcal{G}^2 dependence in the tunneling regime and is suppressed at contact, suggests that it scales as the square of the prefactor in the *noninteracting* noise, i.e. $S_{2e}^< \sim T^2(1 - T)^2$. To test this hypothesis, we inspect the finite-frequency Fano factor $F(\omega) = \mathcal{S}(\omega)/eI$ which should then scale with the transmission coefficient as

$$F_{1e} \sim 1 - T \quad \text{and} \quad F_{2e} \sim T(1 - T)^2, \quad (16)$$

with the maximum of F_{2e} occurring at $T = 1/3$. The integrated Fano factors shown in Fig. 3(c) are in excellent agreement with our expectations, confirming the anticipated scaling of the $2e$ emission noise. The ratio of the $1e$ and $2e$ emission noise thus scales with the coupling constant and transmission coefficient as $S_{2e}^</math>$

Next, we discuss the emission spectrum shown in Fig. 4 as a function of bias voltage and conductance. As expected, the emission which resembles the LSP spectrum

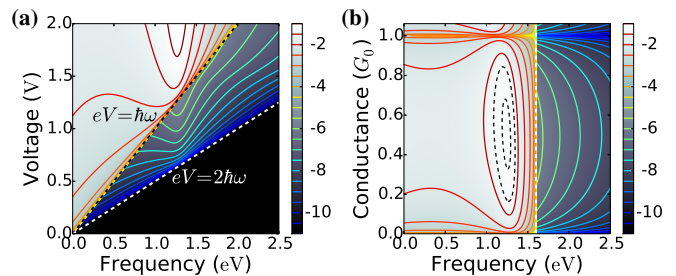


FIG. 4. (Color online) (a) Emission spectrum vs applied voltage for a contact with $T \sim 0.2$. (b) Emission spectrum vs transmission coefficient at $V = 1.6$ V. The plots show the emission rate $\Gamma_{\text{rad}}(\omega) \propto -\text{Im}D^<(\omega)$ in units of γ_{rad} on a logarithmic scale. Parameters: $\omega_{\text{pl}} = 1.5$ eV, $\gamma_0 = 0.2$ eV, $M = 0.1$, $\Gamma_{\text{tip}} = 10$ eV.

has a dominant $1e$ component which is driven by the *noninteracting* quantum noise, and a weaker $2e$ component driven by the higher-order quantum noise. Due to the predicted T dependence of the quantum noise, both the $1e$ and $2e$ emission peak at $\mathcal{G} \sim 0.5 G_0$ and are strongly reduced at $\mathcal{G} \sim G_0$. This counter intuitive behavior at perfect transmission where the current is maximized and one naively would expect the same for the emission, is a unique fingerprint of the quantum noise origin.

The tunneling-induced damping of the LSP associated with the dissipative part of the AC conductance gives rise to an additional spectral broadening $\gamma_{\text{el}} = -2\text{Im}\Pi^{\nabla}$. In the large Γ -limit and to lowest order in the el-pl interaction, $\text{Re}\mathcal{G}(\omega) = G_0 T$ and $\gamma_{\text{el}} = 8\omega/\pi M^2 T$. Contrary to the emission noise, it does not vanish at $T = 1$ and is independent of the bias voltage. Due to the nondissipative part of the AC conductance (real part of the self-energy) the LSP resonance redshifts (~ 0.1 eV) with increasing conductance in Fig. 4(b). Similar spectral features have been observed in subnanometer plasmonic contacts [28, 51], though the importance of tunneling versus other mechanisms is unclear [52–56]. Our findings indicate that electron tunneling plays a nonnegligible role in the quantum regime.

Finally, in Fig. 3(d) we show the calculated $2e$ emission yield, defined as emission per current, as a function of conductance together with the experimental $2e$ photon yield from Ref. [6]. Compared to the Fano factor in Fig. 3(c), the above-mentioned spectral changes result in a slight left shift of the curve for the yield. The agreement with the experimental $2e$ yield is very good, indicating that we have identified the mechanism responsible for $2e$ emission. At $\mathcal{G} \sim G_0$, however, the experimental yields do not show complete suppression (see Ref. [6]). This discrepancy can be due to experimental factors such as: (i) imperfect or additional transmission channels [6], and/or (ii) changes in the LSP mode and el-pl coupling as the tip-substrate distance is reduced [57].

Summary.—To summarize, we have presented a frame-

work based on the Keldysh GF formalism for the description of light emission from plasmonic contacts and established the connection between the quantum noise and AC conductance of the contact and the light emission. Studying a generic contact model, we have identified a plasmon-induced el-el interaction associated with the higher-order quantum noise as the mechanisms behind the experimentally observed above-threshold emission [6, 7]. Our approach, which can be generalized to more complex situations, paves the way for a better understanding of the effect of interactions on light emission and quantum noise in atomic-scale and molecular contacts.

We would like to thank W. Belzig, T. Novotný, M. Galperin, N. A. Mortensen, J. Paaske and M. Brandbyge for fruitful discussions, R. Berndt for providing us with the original data from Ref. 6 and M. H. Fischer for comments on the manuscript. This research was supported by the Israel Science Foundation, the Israel-US Binational Science Foundation (grant No. 2011509), and the European Science Council (FP7/ERC grant No. 226628). AN thanks the Physics Department at FUB and SFB 658 for hospitality during the time this work was completed. KK acknowledges support from the Vilum and Carlsberg Foundations.

* cosby@fys.ku.dk

- [1] N. Agraït, A. Levy Yeyati, and J. M. van Ruitenbeek, “Quantum properties of atomic-sized conductors,” *Physics Reports* **377**, 81 (2003).
- [2] L. Olesen, E. Laegsgaard, I. Stensgaard, F. Besenbacher, J. Schiøtz, P. Stoltze, K. W. Jacobsen, and J. K. Nørskov, “Quantized conductance in an atom-sized point contact,” *Phys. Rev. Lett.* **72**, 2251 (1994).
- [3] H. E. van den Brom and J. M. van Ruitenbeek, “Quantum suppression of shot noise in atom-size metallic contacts,” *Phys. Rev. Lett.* **82**, 1526 (1999).
- [4] N. Agraït, C. Untiedt, G. Rubio-Bollinger, and S. Vieira, “Electron transport and phonons in atomic wires,” *Phys. Rev. Lett.* **88**, 216803 (2002).
- [5] M. Kumar, R. Avriller, A. L. Yeyati, and J. M. van Ruitenbeek, “Detection of vibration-mode scattering in electronic shot noise,” *Phys. Rev. Lett.* **108**, 146602 (2012).
- [6] N. L. Schneider, G. Schull, and R. Berndt, “Optical probe of quantum shot-noise reduction at a single-atom contact,” *Phys. Rev. Lett.* **105**, 026601 (2010).
- [7] G. Schull, N. Néel, P. Johansson, and R. Berndt, “Electron-plasmon and electron-electron interactions at a single atom contact,” *Phys. Rev. Lett.* **102**, 057401 (2009).
- [8] G. B. Lesovik and R. Loosen, “On the detection of finite-frequency current fluctuations,” *Pis’ma Zh. Eksp. Teor. Fiz.* **65**, 280 (1997), [*JETP Lett.* **65**, 295 (1997)].
- [9] R. Aguado and L. P. Kouwenhoven, “Double quantum dots as detectors of high-frequency quantum noise in mesoscopic conductors,” *Phys. Rev. Lett.* **84**, 1986 (2000).
- [10] U. Gavish, Y. Levinson, and Y. Imry, “Detection of quantum noise,” *Phys. Rev. B* **62**, 10637 (2000).
- [11] C. W. J. Beenakker and H. Schomerus, “Counting statistics of photons produced by electronic shot noise,” *Phys. Rev. Lett.* **86**, 700 (2001).
- [12] Z. C. Dong, X. L. Zhang, H. Y. Gao, Y. Luo, C. Zhang, L. G. Chen, R. Zhang, X. Tao, Y. Zhang, J. L. Yang, and J. G. Hou, “Generation of molecular hot electroluminescence by resonant nanocavity plasmons,” *Nature Phot.* **4**, 50 (2010).
- [13] N. L. Schneider, J. T. Lü, M. Brandbyge, and R. Berndt, “Light emission probing quantum shot noise and charge fluctuations at a biased molecular junction,” *Phys. Rev. Lett.* **109**, 186601 (2012).
- [14] M. Galperin and A. Nitzan, “Molecular optoelectronics: the interaction of molecular conduction junctions with light,” *Phys. Chem. Chem. Phys.* **14**, 9421 (2012).
- [15] J.-T. Lü, R. Bjerregaard Christensen, and M. Brandbyge, “Light emission and finite-frequency shot noise in molecular junctions: From tunneling to contact,” *Phys. Rev. B* **88**, 045413 (2013).
- [16] G. Reecht, F. Scheurer, V. Speisser, Y. J. Dappe, F. Mathevet, and G. Schull, “Electroluminescence of a polythiophene molecular wire suspended between a metallic surface and the tip of a scanning tunneling microscope,” *Phys. Rev. Lett.* **112**, 047403 (2014).
- [17] E. Zakka-Bajjani, J. Ségala, F. Portier, P. Roche, D. C. Glattli, A. Cavanna, and Y. Jin, “Experimental test of the high-frequency quantum shot noise theory in a quantum point contact,” *Phys. Rev. Lett.* **99**, 236803 (2007).
- [18] E. A. Rothstein, O. Entin-Wohlman, and A. Aharony, “Noise spectra of a quantum dot,” *Phys. Rev. B* **79**, 075307 (2009).
- [19] A. A. Clerk, M. H. Devoret, S. M. Girvin, F. Marquardt, and R. J. Schoelkopf, “Introduction to quantum noise, measurement, and amplification,” *Rev. Mod. Phys.* **82**, 1155 (2010).
- [20] J. Basset, H. Bouchiat, and R. Deblock, “Emission and absorption quantum noise measurement with an on-chip resonant circuit,” *Phys. Rev. Lett.* **105**, 166801 (2010).
- [21] A. V. Lebedev, G. B. Lesovik, and G. Blatter, “Statistics of radiation emitted from a quantum point contact,” *Phys. Rev. B* **81**, 155421 (2010).
- [22] M. Hofheinz, F. Portier, Q. Baudouin, P. Joyez, D. Vion, P. Bertet, P. Roche, and D. Esteve, “Bright side of the Coulomb blockade,” *prl* **106**, 217005 (2011).
- [23] C. P. Orth, D. F. Urban, and A. Komnik, “Finite-frequency noise properties of the nonequilibrium Anderson impurity model,” *Phys. Rev. B* **86**, 125324 (2012).
- [24] R. Zamoum, A. Crépieux, and I. Safi, “One-channel conductor coupled to a quantum of resistance: Exact ac conductance and finite-frequency noise,” *Phys. Rev. B* **85**, 125421 (2012).
- [25] C. Altimiras, O. Parlavecchio, P. Joyez, D. Vion, P. Roche, D. Esteve, and F. Portier, “Dynamical Coulomb blockade of shot noise,” *Phys. Rev. Lett.* **112**, 236803 (2014).
- [26] F. Xu, C. Holmqvist, and W. Belzig, “Overbias light emission due to higher-order quantum noise in a tunnel junction,” *Phys. Rev. Lett.* **113**, 066801 (2014).
- [27] J.-C. Fergues, C. Lupien, and B. Reulet, “Emission of microwave photon pairs by a tunnel junction,” *Phys. Rev. Lett.* **113**, 043602 (2014).

- [28] K. J. Savage, M. M. Hawkeye, R. Esteban, A. G. Borisov, J. Aizpurua, and J. J. Baumberg, “Revealing the quantum regime in tunnelling plasmonics,” *Nature* **491**, 574 (2012).
- [29] P. Bharadwaj, A. Bouhelier, and L. Novotny, “Electrical excitation of surface plasmons,” *Phys. Rev. Lett.* **106**, 226802 (2011).
- [30] M. S. Tame, K. R. McEnery, Ş. K. Özdemir, J. Lee, S. A. Maier, and M. S. Kim, “Quantum plasmonics,” *Nature Phys.* **9**, 329 (2013).
- [31] G. Hoffmann, R. Berndt, and P. Johansson, “Two-electron photon emission from metallic quantum wells,” *Phys. Rev. Lett.* **90**, 046803 (2003).
- [32] J. Tobiska, J. Danon, I. Snyman, and Yu. V. Nazarov, “Quantum tunneling detection of two-photon and two-electron processes,” *Phys. Rev. Lett.* **96**, 096801 (2006).
- [33] N. L. Schneider, P. Johansson, and R. Berndt, “Hot electron cascades in the scanning tunneling microscope,” *Phys. Rev. B* **87**, 045409 (2013).
- [34] J. Rammer and H. Smith, “Quantum field-theoretical methods in transport theory of metals,” *Rev. Mod. Phys.* **58**, 323 (1986).
- [35] H. Haug and A.-P. Jauho, *Quantum Kinetics in Transport and Optics of Semiconductors* (Springer, Berlin, 1998).
- [36] R. W. Rendell, D. J. Scalapino, and B. Mühlischlegel, “Role of local plasmon modes in light emission from small-particle tunnel junctions,” *Phys. Rev. Lett.* **41**, 1746 (1978).
- [37] P. Johansson, R. Monreal, and P. Apell, “Theory for light emission from a scanning tunneling microscope,” *Phys. Rev. B* **42**, 9210 (1990).
- [38] R. Berndt, J. K. Gimzewski, and P. Johansson, “Inelastic tunneling excitation of tip-induced plasmon modes on noble-metal surfaces,” *Phys. Rev. Lett.* **67**, 3796 (1991).
- [39] A. García-Martín, D. R. Ward, D. Natelson, and J. C. Cuevas, “Field enhancement in subnanometer metallic gaps,” *Phys. Rev. B* **83**, 193404 (2011).
- [40] P. Johansson, “Light emission from a scanning tunneling microscope: Fully retarded calculation,” *Phys. Rev. B* **58**, 10823 (1998).
- [41] G. D. Mahan, *Many-particle Physics*, 3rd ed. (Springer, 2010).
- [42] See Supplemental Material [url].
- [43] We use the symbols S and \mathcal{S} for the correlation function in units of eV and $\frac{e^2}{s}$, respectively. The replacement $\frac{1}{2\pi} \leftrightarrow \frac{e^2}{h}$ switches between the two.
- [44] This follows from the relations $S^r - S^a = S^> - S^<$, $S^>(\omega) = S^<(-\omega)$ and $D^>(\omega) = D^<(-\omega)$.
- [45] U. Gavish, Y. Imry, and Y. Levinson, “Quantum noise, detailed balance and Kubo formula in nonequilibrium quantum systems,” in *Proceedings of the 2001 Rencontres de Moriond: Electronic Correlations: from Mesoscale to Nanophysics*, edited by T. Martin, G. Montambaux, and J. Tran Thanh Van (EDP Science, Lesulis, 2001) arXiv:cond-mat/0211681.
- [46] D. J. Scalapino, S. R. White, and S. Zhang, “Insulator, metal, or superconductor: The criteria,” *Phys. Rev. B* **47**, 7995 (1993).
- [47] As opposed to charge fluctuations of the contact, $\Delta I = I_{\text{tip}} + I_{\text{sub}}$, which would be the case if $M_{\text{tip}} = M_{\text{sub}}$.
- [48] Y. M. Blanter and M. Büttiker, “Shot noise in mesoscopic conductors,” *Phys. Rep.* **336**, 1 (2000).
- [49] The factor of 4 in Eq. (15) stems from the fact that the total noise, $S^< = \sum_{\alpha\beta} S_{\alpha\beta}^<$, is considered.
- [50] A. Zee, *Quantum Field Theory in a Nutshell*, 2nd ed. (Princeton University Press, Princeton, 2010).
- [51] J. A. Scholl, A. García-Etxarri, A. Leen Koh, and J. A. Dionne, “Observation of quantum tunneling between two plasmonic nanoparticles,” *Nano. Lett.* **13**, 564 (2013).
- [52] P. Song, P. Nordlander, and S. Gao, “Quantum mechanical study of the coupling of plasmon excitations to atomic-scale electron transport,” *J. Chem. Phys.* **134**, 074701 (2011).
- [53] R. Esteban, A. G. Borisov, P. Nordlander, and Javier Aizpurua, “Bridging quantum and classical plasmonics with a quantum-corrected model,” *Nature Comm.* **3**, 825 (2012).
- [54] N. Asger Mortensen, S. Raza, M. Wubs, T. Søndergaard, and S. I. Bozhevolnyi, “A generalized non-local optical response theory for plasmonic nanostructures,” *Nature Comm.* **5**, 3809 (2014).
- [55] T. V. Teperik, P. Nordlander, J. Aizpurua, and A. G. Borisov, “Robust subnanometric plasmon ruler by rescaling of the nonlocal optical response,” *Phys. Rev. Lett.* **110**, 263901 (2013).
- [56] T. V. Teperik, P. Nordlander, J. Aizpurua, and A. G. Borisov, “Quantum effects and nonlocality in strongly coupled plasmonic nanowire dimers,” *Optics Express* **21**, 27306 (2013).
- [57] J. Aizpurua, G. Hoffmann, S. P. Apell, and R. Berndt, “Electromagnetic coupling on an atomic scale,” *Phys. Rev. Lett.* **89**, 156803 (2002).

Supplemental material for “*Theory of light emission from quantum noise in plasmonic contacts: above-threshold emission from higher-order electron-plasmon scattering*”

Kristen Kaasbjerg^{1,2} and Abraham Nitzan²

¹*Department of Condensed Matter Physics, Weizmann Institute of Science, Rehovot, Israel 76100*

²*School of Chemistry, The Sackler Faculty of Exact Sciences, Tel Aviv University, Tel Aviv 69978, Israel*
(Dated: January 25, 2015)

I. LSP GREEN'S FUNCTION

The central object of interest for our description of plasmonic light emission from biased STM contacts, is the contour-ordered GF for the localized surface-plasmon polariton (LSP) of the contact represented by the quantized vector potential

$$\mathbf{A}(\mathbf{r}) = \boldsymbol{\xi}_{\text{pl}}(\mathbf{r}) \sqrt{\frac{\hbar}{2\Omega\epsilon_0\omega_{\text{pl}}}} (a^\dagger + a), \quad (1)$$

where Ω is a quantization volume and $\boldsymbol{\xi}_{\text{pl}}$ is the mode vector. The contour-ordered GF is defined by

$$D(\tau, \tau') = -i\langle T_c A(\tau) A(\tau') \rangle, \quad (2)$$

where $A = a + a^\dagger$ and T_c is the time-ordering operator on the Keldysh contour. In the presence of interactions, it obeys the Dyson equation

$$D(\tau, \tau') = d_0(\tau, \tau') + \int d\tau_1 \int d\tau_2 \times d_0(\tau, \tau_1) \Pi(\tau_1, \tau_2) D(\tau_2, \tau'), \quad (3)$$

where d_0 is the *bare* GF and Π is the *irreducible* self-energy.

A. Electron-plasmon self-energy

In order to establish an *exact* expression for the el-pl self-energy, we start from the perturbation expansion of

the LSP GF in terms of the S -matrix on the Keldysh contour,

$$S_c = T_c \exp \left[-i \int_c d\tau_1 V(\tau_1) \right], \quad (4)$$

where

$$V = \int d\mathbf{r} \mathbf{j}_{\text{el}}(\mathbf{r}) \cdot \mathbf{A}(\mathbf{r}) \quad (5)$$

is the el-pl interaction accounting for the interaction with the tunnel current, $\mathbf{j}_{\text{el}} = \mathbf{j}^\nabla + \mathbf{j}^A$, which is a sum of paramagnetic and diamagnetic components. As explained in the main text, we here neglect the diamagnetic component and focus on the paramagnetic self-energy, Π^∇ , which governs the excitation dynamics of the LSP.

Introducing the current operator

$$j = \sqrt{\frac{\hbar}{2V\epsilon_0\omega_{\text{pl}}}} \int d\mathbf{r} \boldsymbol{\xi}_{\text{pl}}(\mathbf{r}) \cdot \mathbf{j}^\nabla(\mathbf{r}), \quad (6)$$

the S -matrix expansion of the LSP GF in the paramagnetic interaction can be written

$$\begin{aligned} D(\tau, \tau') &= -i\langle T_c S_c A(\tau) A(\tau') \rangle_0 \\ &= -i \sum_{n=0}^{\infty} \frac{(-i)^n}{n!} \int d\tau_1 \cdots \int d\tau_n \langle T_c A(\tau) V(\tau_1) \cdots V(\tau_n) A(\tau') \rangle_0^{\text{con}} \\ &= -i \sum_{n=0}^{\infty} \frac{(-i)^{2n}}{(2n)!} \int d\tau_1 \cdots \int d\tau_{2n} \langle T_c A(\tau) A(\tau_1) \cdots A(\tau_{2n}) A(\tau') \rangle_0 \langle T_c j(\tau_1) \cdots j(\tau_{2n}) \rangle_0, \end{aligned} \quad (7)$$

where the sum is over connected diagrams and, in the last equality, we have replaced $n \rightarrow 2n$ (the expectation value of an odd number of boson operators is zero, implying that only even orders contribute in the perturbation series).

In order to identify the bosonic self-energy from the perturbation series, the expectation value of the time-ordered

bosonic operators is rewritten as

$$\langle T_c A(\tau) A(\tau_1) \cdots A(\tau_{2n}) A(\tau') \rangle_0 = 2n(2n-1) \langle T_c A(\tau) A(\tau_1) \rangle_0 \langle T_c A(\tau_2) \cdots A(\tau_{2n-1}) \rangle_0 \langle T_c A(\tau_{2n}) A(\tau') \rangle_0 \quad (8)$$

The factor of $2n(2n-1)$ on the right-hand side comes from number of ways two internal times can be paired up with the two external times τ, τ' in the Wick's contraction of the bosonic expectation value. For each pairing τ, τ_n and $\tau', \tau_{n'}$, the contractions of the remaining $2n-2$ internal boson operators are recollected in the uncontracted expectation value.

The GF can now be written

$$D(\tau, \tau') = d_0(\tau, \tau') + \int d\tau_1 \int d\tau_2 d_0(\tau, \tau_1) \Pi^\nabla(\tau_1, \tau_2) d_0(\tau_2, \tau') \quad (9)$$

where the *reducible* self-energy is defined by

$$\begin{aligned} \Pi^\nabla(\tau, \tau') &= i \sum_{n=1}^{\infty} \frac{(-i)^{2n}}{(2n)!} 2n(2n-1) \int d\tau_1 \cdots \int d\tau_{2n-2} \langle T_c j(\tau) j(\tau_1) \cdots j(\tau_{2n-2}) j(\tau') \rangle_0 \langle T_c A(\tau_1) \cdots A(\tau_{2n-2}) \rangle_0 \\ &= -i \sum_{n=0}^{\infty} \frac{(-i)^{2n}}{(2n)!} \int d\tau_1 \cdots \int d\tau_{2n} \langle T_c j(\tau) j(\tau_1) \cdots j(\tau_{2n}) j(\tau') \rangle_0 \langle T_c A(\tau_1) \cdots A(\tau_{2n}) \rangle_0 \\ &\equiv -i S(\tau, \tau'). \end{aligned} \quad (10)$$

Here, we have identified the sum over connected diagrams in the second line as the perturbation expansion of the correlation function $S(\tau, \tau') = \langle T_c \delta j(\tau) \delta j(\tau') \rangle$ where $\delta j = j - \langle j \rangle$. Writing out the correlation function we have $S(\tau, \tau') = \langle T_c j(\tau) j(\tau') \rangle - \langle j \rangle^2$. Here, the last term cancels the disconnected diagrams from the perturbation expansion of the first term which do not appear in the expansion for the LSP GF in Eq. (7).

From the above, it follows trivially that the *irreducible* self-energy is given by

$$\Pi^\nabla(\tau, \tau') \equiv -i S^{\text{irr}}(\tau, \tau'), \quad (11)$$

where S^{irr} is the *irreducible* part of the correlation function S .

B. Self-energy for the contact model

For the simple contact model considered in the main text, the paramagnetic part of the interaction can be written on the form¹

$$V = \sum_{\alpha} M_{\alpha} I_{\alpha} (a^{\dagger} + a) \quad (12)$$

where M_{α} is the coupling constant at lead α and the paramagnetic current operator is defined by

$$I_{\alpha} = i \sum_k \left[t_{\alpha} c_{\alpha k}^{\dagger} d - \text{h.c.} \right], \quad (13)$$

where the sum is over states k in the lead. It is here assumed that the tunnel coupling t_{α} and the coupling constant M_{α} are independent on the state index k .

Repeating the perturbation expansion for the plasmonic GF in the preceding section with the interaction in Eq. (12), we find that the paramagnetic self-energy can be written as a sum over lead components, $\Pi^\nabla = \sum_{\alpha\beta} \Pi_{\alpha\beta}^\nabla$, where

$$\Pi_{\alpha\beta}^\nabla(\tau, \tau') = -i M_{\alpha} M_{\beta} S_{\alpha\beta}^{\text{irr}}(\tau, \tau'), \quad (14)$$

and $S_{\alpha\beta}(\tau, \tau') = \langle T_c \delta I_{\alpha}(\tau) \delta I_{\beta}(\tau') \rangle$ is the *reducible* correlation function with $\delta I_{\alpha} = I_{\alpha} - \langle I_{\alpha} \rangle$.

1. Identities for the self-energy

From the hermitian property of the paramagnetic current operator I_{α} , the following set of identities between the different lead-lead components of the retarded/advanced and lesser/greater self-energies can be derived.

For the retarded/advanced components we have

$$\Pi_{\alpha\beta}^r(\omega) = [\Pi_{\beta\alpha}^a(\omega)]^* = \Pi_{\beta\alpha}^a(-\omega) = [\Pi_{\alpha\beta}^r(-\omega)]^*. \quad (15)$$

For the lesser/greater components,

$$\Pi_{\alpha\beta}^<(\omega) = \Pi_{\beta\alpha}^>(-\omega). \quad (16)$$

In addition, the components of the lesser self-energy in frequency domain are related as

$$[\Pi_{\alpha\beta}^<(\omega)]^* = -\Pi_{\beta\alpha}^<(\omega). \quad (17)$$

Hence, the diagonals $\Pi_{\alpha\alpha}^<$ are purely imaginary while the off-diagonal elements, in general, have both a real and an imaginary part. Note, however, that the real parts of the off-diagonal components cancel each other, implying that the total lesser self-energy becomes purely imaginary.

II. PERTURBATION SERIES FOR THE SELF-ENERGY

The perturbation series and the rules for evaluating the corresponding Feynman diagrams are most easily developed by writing the el-pl interaction (12) on the general form

$$V = \sum_{ij} M_{ij} c_i^\dagger c_j (a^\dagger + a) \quad (18)$$

where $i, j = \alpha, d$ and $\alpha = L, R$ is a composite lead/state index, $\alpha = (\alpha, k)$. With the interaction written on this

form, the el-pl interaction (12) can be represented by the coupling matrix

$$\mathbf{M} = i \begin{pmatrix} 0 & -t_L M_L & -t_R M_R \\ t_L M_L & 0 & 0 \\ t_R M_R & 0 & 0 \end{pmatrix}, \quad (19)$$

in the (d, L, R) basis.

We can now write up the perturbation series for the lead-lead components of the self-energy and get

$$\begin{aligned} \Pi_{\alpha\beta}^\nabla(\tau, \tau') &= -i M_\alpha M_\beta \sum_{n=0}^{\infty} \frac{(-i)^n}{n!} \int d\tau_1 \cdots \int d\tau_n \langle T I_\alpha(\tau) V(\tau_1) \cdots V(\tau_n) I_\beta(\tau') \rangle_0^{\text{con}} \\ &= -i \sum_{ij \in \{\alpha, d\}} \sum_{i'j' \in \{\beta, d\}} M_{ij} M_{i'j'} \sum_{n=0}^{\infty} \frac{(-i)^{2n}}{(2n)!} \int d\tau_1 \cdots \int d\tau_{2n} \sum_{i_1 j_1 \cdots i_{2n} j_{2n}} M_{i_1 j_1} \cdots M_{i_{2n} j_{2n}} \\ &\quad \times \langle T c_i^\dagger(\tau) c_j(\tau) c_{i_1}^\dagger(\tau_1) c_{j_1}(\tau_1) \cdots c_{i_{2n}}^\dagger(\tau_{2n}) c_{j_{2n}}(\tau_{2n}) c_{i'}^\dagger(\tau') c_{j'}(\tau') \rangle_0 \langle T_c A(\tau_1) \cdots A(\tau_{2n}) \rangle_0. \end{aligned} \quad (20)$$

Here the first two sums over i, j and i', j' are associated with the current operators appearing explicitly in the correlation function $S_{\alpha\beta}$.

A. The contact GF

Given the structure of the perturbation series in (20) above, the fundamental building block in the Feynman diagrams for the self-energy is identified as the contact Green's function defined by

$$G_{ij}(\tau, \tau') = -i \langle T_c c_i(\tau) c_j^\dagger(\tau') \rangle_0, \quad (21)$$

where $i, j = \alpha, d$.

In the absence of interactions, i.e. only tunneling between the leads and the level is included, the components of the contact GF are given by

$$G_{dd}(\tau, \tau') = g_d(\tau, \tau') + \int d\tau_1 \int d\tau_2 g_d(\tau, \tau_1) \Sigma(\tau_1, \tau_2) G_{dd}(\tau_2, \tau') \quad (22)$$

$$G_{\alpha d}(\tau, \tau') = \int d\tau_1 t_\alpha g_\alpha(\tau, \tau_1) G_{dd}(\tau_1, \tau') \quad (23)$$

$$G_{d\alpha}(\tau, \tau') = \int d\tau_1 G_{dd}(\tau, \tau_1) t_\alpha^* g_\alpha(\tau_1, \tau') \quad (24)$$

$$G_{\alpha\beta}(\tau, \tau') = \delta_{\alpha\beta} g_\alpha(\tau, \tau') + \int d\tau_1 \int d\tau_2 g_\alpha(\tau, \tau_1) t_\alpha G_{dd}(\tau_1, \tau_2) t_\alpha^* g_\beta(\tau_2, \tau') \quad (25)$$

where $\Sigma = \Sigma_L + \Sigma_R$, $\Sigma_\alpha = \sum_k |t_\alpha|^2 g_\alpha$ is the self-energy due to the coupling to the leads here described within the wide-band limit, and $g_{\alpha/d}$ is the *bare* lead/dot GFs.

B. Feynman rules

The perturbation series for the self-energy in (20) can be represented by the Feynman diagrams familiar from perturbation expansions of other two-particle GFs in the presence of an electron-boson interaction (see Fig. 2 of the main text)². Here, we give the Feynman rules that apply to the present case:

- At order $2n$, draw $2n + 2$ vertices.
- Label each vertex with i, j indices and multiply by M_{ij} .
- Connect vertices with the components of the contact GFs (21) matching the in/out going vertex indices.
- Connect internal vertices with *bare* boson GFs.
- At each vertex, sum over the states of the involved lead. The appearance of $\sum_k t_\alpha / \sum_k t_\alpha^*$ at each vertex, implies that the component of the contact GF entering/exiting the vertex with a lead index can be replaced according to:

$$- G_{\alpha\beta}(\tau, \tau') \rightarrow \delta_{\alpha\beta} \Sigma_\alpha(\tau, \tau') + \int d\tau_1 \int d\tau_2 \Sigma_\alpha(\tau, \tau_1) G_{dd}(\tau_1, \tau_2) \Sigma_\beta(\tau_2, \tau')$$

$$\begin{aligned} & -G_{\alpha d}(\tau, \tau') \rightarrow \int d\tau_1 \Sigma_\alpha(\tau, \tau_1) G_{dd}(\tau_1, \tau') \\ & -G_{d\alpha}(\tau, \tau') \rightarrow \int d\tau_1 G_{dd}(\tau, \tau_1) \Sigma_\alpha(\tau_1, \tau'), \end{aligned}$$

i.e., only the k -summed lead-dot/dot-lead/lead-lead GFs appear in the perturbation series.

- Integrate over all internal contour times.
- Factor of -1 for each fermion loop.
- Factor of $-i \times i^{n+2}$ at order $2n$.

The evaluation of the self-energy (retarded/advanced and lesser/greater) on the real-time axis can be accomplished using Keldysh GFs³.

III. GFS IN KELDYSH SPACE

In a perturbative calculation of the self-energy, it can be advantageous to work with the GFs in Keldysh space spanned by the forward ($-$) and backward ($+$) branches of the Keldysh contour³. The GFs are here expressed as 2×2 matrices (indicated by the \checkmark sign in the following),

$$\check{G} = \begin{pmatrix} G^{--} & G^{-+} \\ G^{+-} & G^{++} \end{pmatrix}, \quad (26)$$

with the components corresponding to the different combinations for the positions of the two time arguments on the contour.

This formulation formally arises from the contour integrals which can be recast to real-time integrals as $\int_c d\tau_i \rightarrow \int_- dt_i^- + \int_+ dt_i^+ = \int dt_i^- - \int dt_i^+$. For an expression on the contour like

$$\begin{aligned} X(\tau, \tau') &= \int_c d\tau_1 d\tau_2 \cdots d\tau_n \\ &\times A_1(\tau, \tau_1) A_2(\tau_1, \tau_2) \cdots A_n(\tau_n, \tau') \end{aligned} \quad (27)$$

which contain n contour integrals, the different real-time components in Keldysh space can hence be obtained as

$$\begin{aligned} X^{\sigma\sigma'}(t, t') &= \sum_{\sigma_1 \sigma_2 \cdots \sigma_n} \eta_1 \eta_2 \cdots \eta_n \int dt_1 dt_2 \cdots dt_n \\ &\times A_1^{\sigma\sigma_1}(t, t_1) A_2^{\sigma_1\sigma_2}(t_1, t_2) \cdots A_n^{\sigma_n\sigma'}(t_n, t'), \end{aligned} \quad (28)$$

where $\sigma_i = -/+$ is the contour branch index and $\eta_i = +/-$ is the accompanying sign. The prefactor in front of the integrals hence keeps track of the overall sign arising from the contour variables residing on the backward branch.

The self-energy due to coupling to leads is

$$\check{\Sigma}_\alpha(\varepsilon) = \begin{pmatrix} \Lambda_\alpha(\varepsilon) & 0 \\ 0 & -\Lambda_\alpha(\varepsilon) \end{pmatrix} + i \begin{pmatrix} \Gamma_\alpha(\varepsilon) [f_\alpha(\varepsilon) - 1/2] & -\Gamma_\alpha(\varepsilon) f_\alpha(\varepsilon) \\ \Gamma_\alpha(\varepsilon) [1 - f_\alpha(\varepsilon)] & \Gamma_\alpha(\varepsilon) [f_\alpha(\varepsilon) - 1/2] \end{pmatrix}. \quad (35)$$

The GF in Keldysh space obeys the Dyson equation

$$\check{G} = \check{g}_0 + \check{g}_0 \check{\sigma}_3 \check{\Sigma} \check{\sigma}_3 \check{G}, \quad (29)$$

where $\check{\sigma}_i$ denotes the Pauli matrices, and can hence be obtained in the usual way as

$$\check{G}^{-1} = \check{g}_0^{-1} - \check{\sigma}_3 \check{\Sigma} \check{\sigma}_3, \quad (30)$$

where g_0 is the *bare* GF and Σ is the self-energy accounting for interactions and couplings to, e.g., external leads. The self-energy is defined as

$$\check{\Sigma} = \begin{pmatrix} \Sigma^{--} & \Sigma^{-+} \\ \Sigma^{+-} & \Sigma^{++} \end{pmatrix}, \quad (31)$$

and the matrix product with the Pauli matrices in (30) adds a minus sign to the off-diagonal elements in order to account for the above-mentioned sign arising from the contour integration in the Dyson equation.

When the *bare* GF \check{g}_0 is diagonal, the full GF is given by

$$\check{G} = \frac{1}{\mathcal{G}} \times \begin{pmatrix} -(g_0^{++})^{-1} + \Sigma^{++} & \Sigma^{-+} \\ \Sigma^{+-} & -(g_0^{--})^{-1} + \Sigma^{--} \end{pmatrix}, \quad (32)$$

where the denominator of the prefactor is given by

$$\mathcal{G} = \Sigma^{-+} \Sigma^{+-} - [(g_0^{--})^{-1} - \Sigma^{--}] [(g_0^{++})^{-1} - \Sigma^{++}] \quad (33)$$

For cases where $\Sigma^{--} = \Sigma^{++}$ and $g_0^{--} = -g_0^{++}$ (see, e.g., below), the denominator of the prefactor simplifies to $\mathcal{G} = \Sigma^r \Sigma^a - (g_0^{--})^{-1} (g_0^{++})^{-1}$.

The above also holds for a bosonic GFs.

In the subsections below, we give expressions for some of the Keldysh space GFs relevant for the present work.

A. GF for electronic level coupled to leads

For a single electronic level the, the GF in the absence of coupling to leads and interactions is given by²

$$\check{g}_0(\varepsilon) = \begin{pmatrix} g^{--}(\varepsilon) & 0 \\ 0 & g^{++}(\varepsilon) \end{pmatrix}. \quad (34)$$

where $g^{--}(\varepsilon) = \frac{1}{\varepsilon - \varepsilon_0 + i \text{sgn}(\varepsilon)}$ and $g^{++}(\varepsilon) = -g^{--}(\varepsilon)$.

With this, we can calculate the GF G_0 for the coupled level and find

$$\check{G}_0(\varepsilon) = \frac{1}{\mathcal{G}(\varepsilon)} \times \begin{pmatrix} \varepsilon - \varepsilon_0 - \sum_{\alpha} \Lambda_{\alpha}(\varepsilon) + i \sum_{\alpha} \Gamma_{\alpha}(\varepsilon) [f_{\alpha}(\varepsilon) - 1/2] & i \sum_{\alpha} \Gamma_{\alpha}(\varepsilon) f_{\alpha}(\varepsilon) \\ -i \sum_{\alpha} \Gamma_{\alpha}(\varepsilon) [1 - f_{\alpha}(\varepsilon)] & -\varepsilon + \varepsilon_0 + \sum_{\alpha} \Lambda_{\alpha}(\varepsilon) + i \sum_{\alpha} \Gamma_{\alpha}(\varepsilon) [f_{\alpha}(\varepsilon) - 1/2] \end{pmatrix}. \quad (36)$$

Note that the off diagonals are given by the usual lesser and greater GFs as expected. In the wide-band limit the denominator of the prefactor reduces to $\mathcal{G}(\varepsilon) = (\varepsilon - \varepsilon_0)^2 + (\Gamma/2)^2$.

B. GF for noninteracting lead

The Keldysh GF for noninteracting lead fermions in equilibrium is given by²

$$\check{g}_k(\varepsilon) = P \frac{1}{\varepsilon - \varepsilon_k} \begin{pmatrix} 1 & 0 \\ 0 & -1 \end{pmatrix} + 2\pi i \delta(\varepsilon - \varepsilon_k) \begin{pmatrix} f(\varepsilon) - 1/2 & f(\varepsilon) \\ -(1 - f(\varepsilon)) & f(\varepsilon) - 1/2 \end{pmatrix}. \quad (37)$$

In the wideband limit, the real part is thrown away.

C. Level-lead GF

The contour-ordered level-lead GF is given by

$$G_{\alpha d}(\tau, \tau') = \int d\tau_1 g_{\alpha}(\tau, \tau_1) t_{\alpha} G_0(\tau_1, \tau'). \quad (38)$$

In Keldysh space it can be written on the form

$$\check{G}_{\alpha d}(\varepsilon) = t_{\alpha} \check{g}_{\alpha}(\varepsilon) \check{\sigma}_3 \check{G}_0(\varepsilon). \quad (39)$$

When multiplied by t_{α}^* and summed over k this can be expressed in terms of the coupling self-energy as

$$\sum_k t_{\alpha}^* \check{G}_{\alpha d}(\varepsilon) = \check{\Sigma}_{\alpha}(\varepsilon) \check{\sigma}_3 \check{G}_0(\varepsilon). \quad (40)$$

D. GF for damped plasmon

The *bare* GF for a plasmon with frequency ω_0 is given by

$$\check{d}_0(\omega) = \begin{pmatrix} d_0^{--}(\omega) & 0 \\ 0 & d_0^{++}(\omega) \end{pmatrix} \quad (41)$$

where $d_0^{--}(\omega) = \frac{1}{\omega - \omega_0 + i\delta} - \frac{1}{\omega + \omega_0 - i\delta} = \frac{2\omega_0}{\omega^2 - \omega_0^2 + i\delta}$ and $d_0^{++}(\omega) = -d_0^{--}(\omega)$.

The self-energy due to damping mechanisms described by a phenomenological damping rate γ is given by

$$\check{\Pi}_{\text{damp}}(\omega) = \begin{pmatrix} -i\gamma [F(\omega) + \text{sgn}(\omega)/2] & i\gamma F(\omega) \\ i\gamma F(-\omega) & -i\gamma [F(\omega) + \text{sgn}(\omega)/2] \end{pmatrix} \quad (42)$$

where $F(\omega) = |n_B(\omega)|$ and $n_B(x) = (e^{\beta x} - 1)^{-1}$ is the Bose-Einstein distribution function ($\beta = 1/k_B T$). For the damped plasmon GF, we then find

$$\check{D}_0(\omega) = \frac{2\omega_0}{\mathcal{D}(\omega)} \begin{pmatrix} \omega^2 - \omega_0^2 - 2\omega_0 i\gamma [F(\omega) + \text{sgn}(\omega)/2] & -2\omega_0 i\gamma F(\omega) \\ -2\omega_0 i\gamma F(-\omega) & -\omega^2 + \omega_0^2 - 2\omega_0 i\gamma [F(\omega) + \text{sgn}(\omega)/2] \end{pmatrix}, \quad (43)$$

where $\mathcal{D}(\omega) = (\omega^2 - \omega_0^2)^2 + 4\omega_0^2(\gamma/2)^2$.

IV. EXPRESSION FOR THE NONINTERACTING QUANTUM NOISE

In the following, we derive an expression for the noninteracting finite-frequency noise for the single-channel contact considered in the main text. We consider here

the total noise

$$S^< = S_{LL}^< + S_{RR}^< - S_{LR}^< - S_{RL}^<, \quad (44)$$

and note that the current-current correlation function $S^<(t, t') = \langle I(t')I(t) \rangle$ is the lesser component of the contour-ordered correlation function $S(\tau, \tau') = \langle T_c I(\tau) I(\tau') \rangle$.

The *noninteracting* quantum noise is given by the

lesser component of the *bare* bubble diagram. Using the Feynman rules for the self-energy above, we can write up

the expression for its lead-lead components and obtain

$$\begin{aligned}
S_{\alpha\beta}(\tau, \tau') &= \langle T_c I_\alpha(\tau) I_\beta(\tau') \rangle_0 \\
&= - \left[t_\alpha^* t_\beta^* G_{\alpha d}(\tau, \tau') G_{\beta d}(\tau', \tau) + t_\alpha t_\beta G_{d\beta}(\tau, \tau') G_{d\alpha}(\tau', \tau) - t_\alpha^* t_\beta G_{\alpha\beta}(\tau, \tau') G_{dd}(\tau', \tau) - t_\alpha t_\beta^* G_{dd}(\tau, \tau') G_{\beta\alpha}(\tau', \tau) \right] \\
&= \left(\delta_{\alpha\beta} \Sigma_\alpha(\tau, \tau') + \int d\tau_1 \int d\tau_2 \Sigma_\alpha(\tau, \tau_1) G_{dd}(\tau_1, \tau_2) \Sigma_\beta(\tau_2, \tau') \right) G_{dd}(\tau', \tau) \\
&\quad + G_{dd}(\tau, \tau') \left(\delta_{\alpha\beta} \Sigma_\alpha(\tau', \tau) + \int d\tau_1 \int d\tau_2 \Sigma_\beta(\tau', \tau_1) G_{dd}(\tau_1, \tau_2) \Sigma_\alpha(\tau_2, \tau) \right) \\
&\quad - \int d\tau_1 \Sigma_\alpha(\tau, \tau_1) G_{dd}(\tau_1, \tau') \int d\tau_1 \Sigma_\beta(\tau', \tau_1) G_{dd}(\tau_1, \tau) - \int d\tau_1 G_{dd}(\tau, \tau_1) \Sigma_\beta(\tau_1, \tau') \int d\tau_1 G_{dd}(\tau', \tau_1) \Sigma_\alpha(\tau_1, \tau).
\end{aligned} \tag{45}$$

Taking the lesser component of this expression, carrying out the transition to the real-time axis (using either Langreth conversion rules⁴ or Keldysh GFs) and moving to frequency domain, we find that the finite-frequency noise can be expressed in terms of the energy-dependent transmission function

$$T(\varepsilon) = \frac{\Gamma_L \Gamma_R}{(\varepsilon - \varepsilon_0)^2 + \Gamma^2/4} \tag{46}$$

as

$$\begin{aligned}
S^<(\omega) &= \int \frac{d\varepsilon}{2\pi} \left[4T(\varepsilon) (1 - T(\varepsilon + \omega)) \sum_{\alpha \neq \beta} f_\alpha(\varepsilon + \omega) (1 - f_\beta(\varepsilon)) + 4T(\varepsilon) T(\varepsilon + \omega) \sum_{\alpha} f_\alpha(\varepsilon + \omega) (1 - f_\alpha(\varepsilon)) \right. \\
&\quad \left. + \frac{1}{\Gamma_L \Gamma_R} T(\varepsilon) T(\varepsilon + \omega) \sum_{\alpha\beta} f_\alpha(\varepsilon + \omega) (1 - f_\beta(\varepsilon)) \left(\delta_{\alpha\beta} \frac{\Gamma_\alpha}{\Gamma_{\gamma \neq \alpha}} \omega^2 - (1 - \delta_{\alpha\beta}) (4\varepsilon\omega + 3\omega^2) \right) \right].
\end{aligned} \tag{47}$$

In the limit $\Gamma \gg eV, \omega$, the terms in the second line go to zero. Thus, with the assumption $\Gamma \gg eV, \omega \gg k_B T$ the noise expression simplifies to

$$\begin{aligned}
S^<(\omega) &\approx 4 \int \frac{d\varepsilon}{2\pi} \left[T(1 - T) \sum_{\alpha \neq \beta} f_\alpha(\varepsilon + \omega) (1 - f_\beta(\varepsilon)) + T^2 \sum_{\alpha} f_\alpha(\varepsilon + \omega) (1 - f_\alpha(\varepsilon)) \right] \\
&= \frac{4}{2\pi} \left[T(1 - T) [F(\omega + eV) + F(\omega - eV)] + 2T^2 F(\omega) \right]
\end{aligned} \tag{48}$$

where $T = 4\Gamma_L \Gamma_R / \Gamma^2$ is the transmission coefficient and $F(x) = xn_B(x)$. This is in agreement with previous works^{5,6}. The factor of 4 in front of the parenthesis orig-

inates from the fact that the total noise is considered here.

¹ D. J. Scalapino, S. R. White, and S. Zhang, Phys. Rev. B **47**, 7995 (1993).

² G. D. Mahan, *Many-particle Physics* (Springer, 2010), 3rd ed.

³ J. Rammer and H. Smith, Rev. Mod. Phys. **58**, 323 (1986).

⁴ H. Haug and A.-P. Jauho, *Quantum Kinetics in Transport*

and Optics of Semiconductors (Springer, Berlin, 1998).

⁵ R. Aguado and L. P. Kouwenhoven, Phys. Rev. Lett. **84**, 1986 (2000).

⁶ Y. M. Blanter and M. Büttiker, Phys. Rep. **336**, 1 (2000).